Altered dynamic brain functional connectivity in patients with white matter hyperintensities: a prospective case-control study

yuanyuan Liu (zero960729@163.com)
Anhui Medical University https://orcid.org/0000-0003-2970-1233
Shanshan Cao
Anhui Medical University
Baogen Du
Anhui Medical University
Jun Zhang
Anhui Medical University
Chen Chen
Anhui Medical University
Panpan Hu
Anhui Medical University
Yanghua Tian
Anhui Medical University
Kai Wang
Anhui Medical University
Gong-Jun Ji
Anhui Medical University
Qiang Wei
Anhui Medical University

Research Article

Keywords: white matter hyperintensities, cognitive impairment, dynamic functional connectivity, sliding window, graph theory

Posted Date: May 23rd, 2022

DOI: https://doi.org/10.21203/rs.3.rs-1613542/v1

Abstract

Background

White matter hyperintensities (WMHs) are commonly observed in older adults and are associated with cognitive impairment. Although resting-state functional magnetic resonance imaging studies have explored the mechanisms of cognitive impairment in patients with WMHs, knowledge about the role of dynamic functional connectivity (dFC) is limited in such patients. Our aim is to explore whether the dFC consists in such patients and associates with cognitive impairment.

Methods

We included 36 healthy controls (HCs) and 104 patients with mild (n = 39), moderate n = 37), and severe (n = 28) WMHs. Comprehensive neuropsychological scales were used to assess the cognitive functions. The sliding window approach was used to generate dFC matrices, and graph theory methods were applied to calculate the variability of the network topological properties. Relationships between cognitive functions and abnormal dFC were evaluated by Pearson's correlation.

Results

Patients with WMHs and HCs showed no significant difference in small-world properties. However, there were significant differences in variability of nodal properties between the four groups, which were located within the default mode network (DMN) and cognitive control network (CCN). Correlation analysis revealed that, as the temporal variability of the nodal cluster coefficient increased in the left SMG, the TMT-A time and the AVLT-study score decreased in patients with WMHs. Moreover, as the nodal efficiency of the left Rolandic operculum increased, the MoCA score, the TMT-A and the TMT-B time increased in patients with WMHs.

Conclusions

Our results indicate that dynamic functional connectivity consists in patients with WMHs and associate with executive and memory function.

1. Introduction

Cerebral small vessel disease (CSVD), a group of diseases that affects the small blood vessels in the brain, can present with various symptoms ranging from mild cognitive impairment to dementia (Rensma, van Sloten, Launer, & Stehouwer, 2018). White matter hyperintensities (WMHs) are considered typical imaging characteristic of CSVD, observed upon magnetic resonance imaging (MRI) with the T2 fluid-attenuated inversion recovery (T2-FLAIR) sequence (Wardlaw et al., 2013). Structural MRI studies have

revealed that WMHs disrupt topological properties, leading to cognitive impairment, especially in memory and executive function (van Leijsen et al., 2019). However, visible structural lesions may induce a cascade of events that spread from the initial disrupted structural connectivity via existing white matter tracts, disrupting functional connectivity, as characterized by the coactivation of remote brain regions.

Functional MRI (fMRI) studies have revealed that the “triple-network model” may also be applicable in CSVD, i.e., disruption of the default mode network (DMN), cognitive control network (CCN), and salience network (SN) (Dey, Stamenova, Turner, Black, & Levine, 2016). Functionally, the DMN and CCN play important roles in self-referential and executive function (Breukelaar IA, 2017; Whitfield-Gabrieli & Ford, 2012), respectively, while the SN is considered the ‘dynamic switch’ between the DMN and CCN (Sridharan D, 2008). The integration and segregation of the intrinsic networks are important factors in the maintenance of information processing and basic cognitive functions (Dwyer et al., 2014). Graph theoretical analyses have revealed that WMHs are related to aberrant topological properties between these networks (Cohen & D'Esposito, 2016); however, the poor temporal resolution of such analyses limits their use in representing the underlying brain connectivity over time.

Temporal changes have been investigated by using a series of sliding windows, with the change in dynamic functional connectivity (dFC) being estimated as correlations between components and time courses (Shakil, Lee, & Keilholz, 2016). Alterations in dFC are reportedly associated with several neurological diseases, including Parkinson's disease (PD) and Alzheimer’s disease (AD). For example,dFC have been observed in the early stages of PD (Cordes et al., 2018), and have also been linked to its progression (Kim et al., 2017). Moreover, the dynamic topological properties of connectivity networks have improved the evaluation of AD progression (Jie, Liu, & Shen, 2018) and its prodrome, that is, mild cognitive impairment (MCI) (Wee, Yang, Yap, & Shen, 2016). Such neuroimaging characteristics provide a novel perspective on functional changes, which is crucial in understanding the spatiotemporal alterations of the intrinsic network associated with WMHs.

In this study, we combined the sliding window approach with graph theory to identify the global and nodal topological properties of dFC associated with WMHs. Moreover, comprehensive tests were used to assess cognitive function in multiple cognitive domains in patients with WMHs. We hypothesized that patients with WMHs exhibit dynamic topological properties, which may also be associated with cognitive impairment.

2. Materials And Methods

2.1 Participants

We recruited 104 patients with WMHs and 36 healthy controls (HCs) from the Department of Neurology of the First Affiliated Hospital of Anhui Medical University. We recruited patients aged 40–80 years who had macroscopic CSVD-related WMHs upon T2-FLAIR MRI. We did not include patients with hearing or visual impairments, language or physical movement disorders, MRI contraindications, or claustrophobia.

We excluded patients with a history of alcohol addiction, psychiatric disorders, or tumors; those who participated in the trial of Org 10172 in Acute Stroke Treatment who were suspected of having experienced cardiogenic stroke; and those with intracranial or exracranial stenosis > 50% or intracranial hemorrhage. The HCs were matched to patients with WMHs in terms of age, sex, and years of education. The study was approved by the Ethics Committee of the Anhui Medical University. The work described in this article was carried out in accordance with The Code of Ethics of the World Medical Association (Declaration of Helsinki) for experiments involving humans, as well as the Uniform Requirements for Manuscripts submitted to biomedical journals. Prior to data collection, informed consent was obtained from all participants.

Patients were divided into three categories according to their Fazekas score: mild WMHs (Fazekas score 1–2; n = 39), moderate WMHs (Fazekas score 3–4; n = 37), and severe WMHs (Fazekas score 5–6; n = 28). The Fazekas score consisted of WMHs and periventricular hyperintensity scores, which were calculated according to the Fazekas scale (Fazekas, Chawluk, Alavi, Hurtig, & Zimmerman, 1987). The UBO segmentation algorithm was selected to extract the WMH volume for further control of the grouping (https://cheba.unsw.edu.au/research-groups/neuroimaging/pipeline)(Jiang et al., 2018).

2.2 Neuropsychological assessment

The participants underwent a neuropsychological test battery that included the main cognitive domains, Patient Health Questionnaire-9 (PHQ-9), and Generalized Anxiety Disorde-7 (GAD-7). Overall cognitive function was evaluated by using the Montreal Cognitive Assessment (MoCA) (Nasreddine et al., 2005), while executive, language, and memory functions were estimated by using the Trail Making Test (TMT) (Sacco et al., 2019), Boston Naming Test (BNT) (Cheung, Cheung, & Chan, 2004), and Auditory Verbal Learning Test (AVLT), respectively (Arnáiz et al., 2004).

2.3 MRI parameters

MRI data were collected by using a GE750w 3.0T MRI system (GE Healthcare, Chicago, IL, USA) at the University of Science and Technology of China. During scanning, participants were instructed to close their eyes, and foam pads were used to minimize head motion. The parameters of structural, 3D, T1-weighted imaging were set as follows: repetition time (TR)/echo time (TE)/flip = 8.16 ms/3.18 ms/12°; 188 continuous slices (thickness of 5 mm with no gap, and voxel size = 1 × 1 × 1 mm^3); and field of view = 256 × 256 mm^2. Functional data were obtained by using the following parameters: TR/TE/flip = 2400 ms/30 ms/90°; matrix size = 64 × 64 px^2; field of view = 192 × 192 mm^2; 46 continuous slices (thickness of 3 mm with no gap, and voxel size = 3 × 3 × 3 mm^3).

2.4 fMRI data processing

All functional images were preprocessed by using the DPABI toolbox (http://rfmri.org/dpabi) (Yan, Wang, Zuo, & Zang, 2016) and SPM8 software (https://www.fil.ion.ucl.ac.uk/spm). The first 10 time points were discarded, and the remaining images were subjected to slice timing and realignment. When the subjects underwent MRI, the quality control was carried out on the head motion (exceeding 3° of rotation or 3 mm

of translation in any dimension), so no subjects were discarded. The eligible images were co-registered to functional images; segmented into gray matter, white matter (WM), and cerebrospinal fluid (CSF) (Ashburner, 2007); and normalized to the Montreal Neurological Institute space. Finally, in the time series of each voxel of each resulting image, the linear trends as well as the WM and CSF signals were removed, and 24 head-motion parameters were regressed (Yan et al., 2013).

2.5 Temporal network construction

We used the Dynamic BC toolbox (Liao et al., 2014) to apply the sliding window approach for extraction of the time series and calculation of the Pearson's correlation coefficients between all pairs of nodes in each window. According to that in previous studies, a window length of 50 TR (120 s) with a step size of 5 TR (12 s) was chosen for estimation of different time series, and each time series was divided into 32 windows. Automated anatomical labeling (Tzourio-Mazoyer et al., 2002) was used to generate whole-brain functional connectivity matrices for each participant. Network edges were defined by using a sparsity threshold ranging from 0.05 to 0.5 in steps of 0.05, and individual correlation matrices were transformed into a binary format.

2.6 Network properties

At each sparsity threshold, we chose a series of graph metrics, including small-world, global, and nodal properties, for estimation of the brain graphs in each pairwise functional connectivity matrix for all sliding windows for all subjects. All graph metrics were computed by using the GRETNA toolbox (http://www.nitrc.org/projects/gretna/)(Wang et al., 2015).

2.6.1 Small-world properties

We calculated small-world properties for all individual networks as global network properties (Bullmore & Sporns, 2009). A small-world network may be defined as a locally compact, clustered network with a relatively short path length between nodes, permitting optimum communication between the nodes in the network (Liu et al., 2008).

2.6.2 Nodal properties

The nodal properties we focused on were degree centrality, betweenness centrality, the nodal clustering coefficient, and nodal efficiency (Rubinov & Sporns, 2010). These properties are the most common indicators with which to judge the degree of information transmission of key nodes at different levels.

2.7 Statistical analysis

Demographic and neuropsychological data were analyzed by using IBM SPSS Statistics for Windows, version 22.0 (IBM Corp., Armonk, NY, USA). One-way analysis of variance was used to assess differences in age, years of education, and neuropsychological test scores, and the chi-square test was used to determine differences in sex, hypertension, diabetes, hyperlipidemia, smoking history, and drinking history among groups (statistically significant at $P < 0.05$). Differences in network properties were assessed by

using one-way analysis of variance (age, sex, and years of education were used as the calibration control variables) and false discovery rate (FDR) correction (statistically significant at a corrected $P < 0.05$). We investigated the relationship between network properties and neuropsychological tests by performing a Pearson's correlation test and FDR correction (statistically significant at a corrected $P < 0.05$).

3. Results

3.1 Demographics, risk factors, and neuropsychological test results

There were no significant differences in age, sex, or years of education between these groups (Table 1). Compared with HCs, patients with WMHs showed poor performance in all neuropsychological assessments (Table 2).

Table 1
Demographic and neuroimaging manifestations

	HC(n = 36)	Mild WMHs(n = 39)	Moderate WMHs(n = 37)	Severe WMHs(n = 28)	F/χ2	*P* value
Age,years [mean (SD)]	60.58 ± 5.98	63.77 ± 8.23	65.08 ± 10.03	65.04 ± 6.90	2.424[b]	0.068
Female,n (%)	18 (50.0%)	16 (41.0%)	14 (37.8%)	16 (57.1%)	3.011[a]	0.390
Education,years [mean (SD)]	9.31 ± 3.32	8.41 ± 4.16	8.00 ± 3.84	7.75 ± 3.88	1.083[b]	0.359
Hypertension,n (%)	8 (22.2%)	21 (53.8%)	22 (59.5%)	21 (75.0%)	19.568[a]	< 0.001 ***
Diabetes,n (%)	2 (5.6%)	8 (20.5%)	7 (18.9%)	4 (14.3%)	3.905[a]	0.272
Hyperlipidemia,n (%)	8 (22.2%)	10 (25.6%)	9 (24.3%)	8 (28.6%)	0.356[a]	0.949
Smoking history,n (%)	9 (25.0%)	18 (46.2%)	15 (40.5%)	11 (39.3%)	3.808[a]	0.283
Drinking history,n (%)	12 (33.3%)	9 (23.1%)	16 (43.2%)	12 (42.9%)	4.346[a]	0.226
Fazekas	0.00 ± 0.00	1.64 ± 0.49	3.59 ± 0.50	5.43 ± 0.50	958.855[b]	< 0.001 ***
WMHs volume	/	11457.35 ± 12493.05	18067.56 ± 10873.84	30658.380 ± 12033.91	21.696[b]	< 0.001 ***
Lacunes	0.00 ± 0.00	0.51 ± 0.91	0.89 ± 1.29	0.79 ± 1.23	5.626[b]	0.001 **
Microbleeds	0.31 ± 0.59	2.26 ± 3.61	1.50 ± 2.35	6.29 ± 14.96	3.389[b]	0.021 *

[a]Chi-square test; [b] One-way analysis of variance

Abbreviations: HC, healthy control; WMHs, white matter hyperintensities; SD, standard deviation;

*** significant at 0.001 level, ** significant at 0.01 level and * significant at 0.05 level (2-tailed).

Table 2
Neuropsychological tests

	HC(n = 36)	Mild WMHs(n = 39)	Moderate WMHs(n = 37)	Severe WMHs(n = 28)	F	*P* value
MoCA	22.33 ± 3.09	21.16 ± 4.32	21.06 ± 3.79	17.81 ± 4.91	6.850	< 0.001 ***
AVLT-study	8.15 ± 1.59	7.63 ± 2.24	7.31 ± 1.52	6.55 ± 2.00	3.776	0.012 *
AVLT-immediate	9.40 ± 2.30	8.17 ± 3.84	7.88 ± 2.65	6.17 ± 3.27	5.320	0.002 **
AVLT-delay	9.06 ± 2.41	7.95 ± 3.76	7.31 ± 2.67	6.50 ± 3.13	3.731	0.013 *
AVLT-recognition	13.63 ± 1.33	13.53 ± 3.68	13.16 ± 1.87	11.13 ± 3.62	4.734	0.004 **
TMT-A	63.34 ± 24.76	80.72 ± 33.12	79.12 ± 33.73	105.82 ± 37.72	8.233	< 0.001 ***
TMT-B	129.65 ± 44.44	155.35 ± 70.69	158.16 ± 73.16	207.55 ± 81.24	6.301	0.001 **
BNT	13.94 ± 0.98	12.89 ± 1.54	13.25 ± 1.68	12.74 ± 1.40	4.797	0.003 **
PHQ-9	3.31 ± 4.78	3.74 ± 4.56	5.00 ± 4.62	7.39 ± 5.81	4.272	0.006 **
GAD-7	2.40 ± 3.24	2.61 ± 4.10	2.81 ± 3.43	5.29 ± 5.48	3.282	0.023 *
Data are mean ± SD						
Abbreviations: HC, healthy control; WMHs, white matter hyperintensities; SD, standard deviation; MoCA, Montreal Cognitive Assessment; AVLT, Chinese Auditory Learning Test; TMT, Trial Making Test; BNT, Boston Naming Test; PHQ, Patient Health Questionnaire; GAD, Generalized Anxiety Disorder.						
Volumes are in cubic millimeters.						
*** significant at 0.001 level, ** significant at 0.01 level and * significant at 0.05 level (2-tailed).						

3.2 Network properties

There were no significant differences in small-world properties between patients with WMHs and HCs. However, there were significant differences in the variability of nodal properties (FDR corrected $P < 0.05$) between the four groups. The betweenness centrality differed among the four groups in bilateral rectus gyri, right inferior occipital lobe, right paracentral lobule, right dorsolateral superior frontal gyrus, and left orbital part of the superior frontal gyrus (Fig. 1). Nodal efficiencies were altered in bilateral Rolandic

opercula, as well as in right superior frontal gyrus, right medial orbital part of superior frontal gyrus, right superior temporal gyrus, and left postcentral gyrus (Fig. 2). The nodal clustering coefficient exhibited high variability in bilateral cunei and medial orbital parts of both superior frontal gyrus, as well as in right superior occipital gyrus, right middle occipital gyrus, right inferior occipital lobe, left superior frontal gyrus, and left supramarginal gyrus (SMG) (Fig. 3).

3.3 Relationship between network properties and cognitive function

Correlation analysis revealed that, as the temporal variability of the nodal cluster coefficient increased in the left SMG, the TMT-A time gradually increased (r = 0.272, FDR corrected P = 0.05), the AVLT-study score gradually decreased (r = − 0.247, FDR corrected P = 0.042) in patients with WMHs (Fig. 4). Moreover, as the nodal efficiency of the left Rolandic operculum increased, the MoCA score gradually decreased (r = − 0.281, FDR corrected P = 0.012), the TMT-A time gradually increased (r = 0.346, FDR corrected P = 0.005), and the TMT-B time gradually increased (r = 0.315, FDR corrected P = 0.008) in patients with WMHs (Fig. 5).

4. Discussion

In this study, the sliding window and graph theory approaches were combined for the identification of alterations in the dFC of patients with WMHs. We discovered that patients with WMHs exhibited higher temporal variability than HCs in nodal properties, particularly in superior frontal gyrus and left supramarginal gyrus (SMG),which belong to the CCN and DMN, but that small-world properties did not differ between these groups. Furthermore, altered nodal characteristics were strongly associated with cognitive impairment in patients with WMHs.

Small-world properties of dFC were not altered in patients with WMHs, suggesting that the integration of the brain functional network remained relatively stable over time. However, the temporal variability of nodal properties was increased in patients with WMHs. Generally, dFC based on resting-state MRI data reflect the spatiotemporal volatility of information among brain regions that occurs in continuous sliding windows. Thus, the higher temporal variability of the nodal properties of these regions in patients with WMHs compared to HCs in our study suggests asynchronicity in their information transmission with other brain regions. Previous exploration of dFC revealed a tight association between stable dFC and underlying anatomical connections (Liégeois et al., 2016). In fact, the functional connections in the brain network influence each other at the spatiotemporal level, and intricate brain functions depend on integration and separation among functionally specialized neural circuits (Knyazev, Slobodskoi-Plyusnin, Savost'yanov, Levin, & Bocharov, 2010) Asynchronicity of the brain regions may impede the transmission of information within and/or between brain networks (Sibille, Morris, Kota, & Lewis, 2011). Notably, many studies have revealed the wide array of pathological connectivity in patients with WMHs (Dey et al., 2016). Patients with WMHs also exhibited low functional connectivity between nodes within the CCN and DMN, which was associated with WMHs severity (Schaefer et al., 2014). Thus, it seems that higher

variability in the dynamic nodal properties of the brain networks reduces their anatomical constraints, and spatially distant functional connections to these pivotal brain regions may lead to further cognitive impairments. It was previously reported that excessive variability in dFC may result in a disconnect among information processing systems (Christoff, Irving, Fox, Spreng, & Andrews-Hanna, 2016). Therefore, higher fluctuations in the dynamic brain network may be suggestive of reduced information processing and maintenance of cognitive function in patients with WMHs.

Conceptually, temporal nodal properties are commonly measured in terms of localized temporal information transmission. Nodal properties refer to the degree of information transmission to other nodes or fault tolerance of a priority node in the subnetwork (Bullmore & Sporns, 2009). An impairment in nodal properties is indicative of a tendency toward a more random organization of the temporal brain networks. Therefore, it seems plausible that the DMN and CCN would exhibit high values in terms of nodal properties (Li et al., 2019). Nodal properties indicative of impaired network efficiency are reportedly related to both white matter damage and cognitive impairment (Lawrence, Chung, Morris, Markus, & Barrick, 2014). As static functional connectivity varies over time, our findings may extend those previous results in that altered dFC was associated with cognitive impairments in patients with WMHs in our study.

Furthermore, we discovered that variation in dFC mainly occurred in the CCN and DMN and was closely associated with executive and memory function in patients with WMHs. The clinical relevance of these correlations can be interpreted according to the functions of these brain regions. The SMG resides in the inferior parietal lobule and is a node of the DMN, establishing complex functional connections between different networks for the regulation of executive functions (Li et al., 2019). Moreover, the SMG can regulate bottom-up attentional orienting and memory retrieval (Rubinstein et al., 2021). The Rolandic operculum regared as the main node of the CCN mediates the encoding and extraction of memories (Kucyi, Hove, Esterman, Hutchison, & Valera, 2017), and is involved in information processing speed (Sridharan, Levitin, & Menon, 2008), which is a key subdomain of cognitive function and is now commonly treated as a pivotal diagnostic indicator for neurocognitive disorders (Torrens-Burton, Basoudan, Bayer, & Tales, 2017). Patients with WMHs exhibit impairments in the domains of cognitive function involving information processing speed, executive function, and memory abilities (Smith et al., 2011). Therefore, increased variability in these brain regions may result in the disruption of executive and memory functions in patients with WMHs. In a previous study, a subset of the alterations located between the DMN and CCN networks was associated with worse cognitive performance in attention, memory, and executive function, which is usually associated with network decoupling (Fox, Zhang, Snyder, & Raichle, 2009). Our results indicate that cognitive deficits in patients with WMHs may be related to a reduction in the normal, negative correlations between the DMN and CCN.

Some limitations that may influence the results should be taken into consideration. First, in addition to WMHs, CSVD is characterized by other neuroimaging manifestations, which may lead to the destruction of different tissue morphology. Second, the sample in our study was small; hence, the results should be considered preliminary, and causality remains to be determined in studies with a larger sample and long-term follow-up.

In conclusion, we combined the sliding window and graph theory approaches to investigate altered dFC in patients with WMHs. Our results indicate that most of the nodal property variability is located within the DMN and CCN, and that the alterations are related to executive and memory function in patients with WMHs. Our study may help neurologists further understand the time-varying of functional imaging and the mechanisms of cognitive impairment in patients with WMHs.

Declarations

Acknowledgements The authors thank the Information Science Laboratory Center of the University of Science and Technology of China for their measurement services.

Author contributions Yuanyuan Liu, Shanshan Cao, and Qiang Wei designed the study. Yuanyuan Liu, Shanshan Cao, Baogen Du, Jun Zhang, Chen Chen collected and analyzed the data.Yuanyuan Guo drafted the manuscript. Panpan Hu, Yanghua Tian, Kai Wang, Gong-Jun Ji, Qiang Wei revised the draft.

Funding This study was supported by the National Key Research and Development Program of China (2021YFC2500104)

Ethical approval All the experiment procedures performed in this study was approved by the ethics committee of the Anhui Medical University and were conducted in accordance with the Helsinki Declaration and its later amendments or comparable ethical standards. All participants provided informed written consent.

Informed consent Written informed consent for publication was obtained from all participants included in the study.

Conflict of interest The authors declare no conflicts of interest.

References

Arnáiz, E., Almkvist, O., Ivnik, R. J., Tangalos, E. G., Wahlund, L. O., Winblad, B., & Petersen, R. C. (2004). Mild cognitive impairment: a cross-national comparison. *J Neurol Neurosurg Psychiatry, 75*(9), 1275-1280. doi:10.1136/jnnp.2003.015032

Ashburner, J. (2007). A fast diffeomorphic image registration algorithm. *Neuroimage, 38*(1), 95-113. doi:10.1016/j.neuroimage.2007.07.007

Breukelaar IA, A. C., Grieve SM, Foster SL, Gomes L, Williams LM, Korgaonkar MS. (2017). Cognitive control network anatomy correlates with neurocognitive behavior: A longitudinal study. *Hum Brain Mapp*. doi:10.1002/hbm.23401

Bullmore, E., & Sporns, O. (2009). Complex brain networks: graph theoretical analysis of structural and functional systems. *Nat Rev Neurosci, 10*(3), 186-198. doi:10.1038/nrn2575

Cheung, R. W., Cheung, M. C., & Chan, A. S. (2004). Confrontation naming in Chinese patients with left, right or bilateral brain damage. *J Int Neuropsychol Soc, 10*(1), 46-53. doi:10.1017/s1355617704101069

Christoff, K., Irving, Z. C., Fox, K. C., Spreng, R. N., & Andrews-Hanna, J. R. (2016). Mind-wandering as spontaneous thought: a dynamic framework. *Nat Rev Neurosci, 17*(11), 718-731. doi:10.1038/nrn.2016.113

Cohen, J. R., & D'Esposito, M. (2016). The Segregation and Integration of Distinct Brain Networks and Their Relationship to Cognition. *J Neurosci, 36*(48), 12083-12094. doi:10.1523/jneurosci.2965-15.2016

Cordes, D., Zhuang, X., Kaleem, M., Sreenivasan, K., Yang, Z., Mishra, V., . . . Cummings, J. L. (2018). Advances in functional magnetic resonance imaging data analysis methods using Empirical Mode Decomposition to investigate temporal changes in early Parkinson's disease. *Alzheimers Dement (N Y), 4*, 372-386. doi:10.1016/j.trci.2018.04.009

Dey, A. K., Stamenova, V., Turner, G., Black, S. E., & Levine, B. (2016). Pathoconnectomics of cognitive impairment in small vessel disease: A systematic review. *Alzheimers Dement, 12*(7), 831-845. doi:10.1016/j.jalz.2016.01.007

Dwyer, D. B., Harrison, B. J., Yücel, M., Whittle, S., Zalesky, A., Pantelis, C., . . . Fornito, A. (2014). Large-scale brain network dynamics supporting adolescent cognitive control. *J Neurosci, 34*(42), 14096-14107. doi:10.1523/jneurosci.1634-14.2014

Fazekas, F., Chawluk, J. B., Alavi, A., Hurtig, H. I., & Zimmerman, R. A. (1987). MR signal abnormalities at 1.5 T in Alzheimer's dementia and normal aging. *AJR Am J Roentgenol, 149*(2), 351-356. doi:10.2214/ajr.149.2.351

Fox, M. D., Zhang, D., Snyder, A. Z., & Raichle, M. E. (2009). The global signal and observed anticorrelated resting state brain networks. *J Neurophysiol, 101*(6), 3270-3283. doi:10.1152/jn.90777.2008

Jiang, J., Liu, T., Zhu, W., Koncz, R., Liu, H., Lee, T., . . . Wen, W. (2018). UBO Detector - A cluster-based, fully automated pipeline for extracting white matter hyperintensities. *Neuroimage, 174*, 539-549. doi:10.1016/j.neuroimage.2018.03.050

Jie, B., Liu, M., & Shen, D. (2018). Integration of temporal and spatial properties of dynamic connectivity networks for automatic diagnosis of brain disease. *Med Image Anal, 47*, 81-94. doi:10.1016/j.media.2018.03.013

Kim, J., Criaud, M., Cho, S. S., Díez-Cirarda, M., Mihaescu, A., Coakeley, S., . . . Strafella, A. P. (2017). Abnormal intrinsic brain functional network dynamics in Parkinson's disease. *Brain, 140*(11), 2955-2967. doi:10.1093/brain/awx233

Knyazev, G. G., Slobodskoi-Plyusnin, Y. Y., Savost'yanov, A. N., Levin, E. A., & Bocharov, A. V. (2010). Reciprocal relationships between the oscillatory systems of the brain. *Neurosci Behav Physiol, 40*(1), 29-

35. doi:10.1007/s11055-009-9227-2

Kucyi, A., Hove, M. J., Esterman, M., Hutchison, R. M., & Valera, E. M. (2017). Dynamic Brain Network Correlates of Spontaneous Fluctuations in Attention. *Cereb Cortex, 27*(3), 1831-1840. doi:10.1093/cercor/bhw029

Lawrence, A. J., Chung, A. W., Morris, R. G., Markus, H. S., & Barrick, T. R. (2014). Structural network efficiency is associated with cognitive impairment in small-vessel disease. *Neurology, 83*(4), 304-311. doi:10.1212/wnl.0000000000000612

Li, C., Li, Y., Zheng, L., Zhu, X., Shao, B., Fan, G., . . . Wang, J. (2019). Abnormal Brain Network Connectivity in a Triple-Network Model of Alzheimer's Disease. *J Alzheimers Dis, 69*(1), 237-252. doi:10.3233/jad-181097

Liao, W., Wu, G. R., Xu, Q., Ji, G. J., Zhang, Z., Zang, Y. F., & Lu, G. (2014). DynamicBC: a MATLAB toolbox for dynamic brain connectome analysis. *Brain Connect, 4*(10), 780-790. doi:10.1089/brain.2014.0253

Liégeois, R., Ziegler, E., Phillips, C., Geurts, P., Gómez, F., Bahri, M. A., . . . Sepulchre, R. (2016). Cerebral functional connectivity periodically (de)synchronizes with anatomical constraints. *Brain Struct Funct, 221*(6), 2985-2997. doi:10.1007/s00429-015-1083-y

Liu, Y., Liang, M., Zhou, Y., He, Y., Hao, Y., Song, M., . . . Jiang, T. (2008). Disrupted small-world networks in schizophrenia. *Brain, 131*(Pt 4), 945-961. doi:10.1093/brain/awn018

Nasreddine, Z. S., Phillips, N. A., Bédirian, V., Charbonneau, S., Whitehead, V., Collin, I., . . . Chertkow, H. (2005). The Montreal Cognitive Assessment, MoCA: a brief screening tool for mild cognitive impairment. *J Am Geriatr Soc, 53*(4), 695-699. doi:10.1111/j.1532-5415.2005.53221.x

Rensma, S. P., van Sloten, T. T., Launer, L. J., & Stehouwer, C. D. A. (2018). Cerebral small vessel disease and risk of incident stroke, dementia and depression, and all-cause mortality: A systematic review and meta-analysis. *Neurosci Biobehav Rev, 90*, 164-173. doi:10.1016/j.neubiorev.2018.04.003

Rubinov, M., & Sporns, O. (2010). Complex network measures of brain connectivity: uses and interpretations. *Neuroimage, 52*(3), 1059-1069. doi:10.1016/j.neuroimage.2009.10.003

Rubinstein, D. Y., Camarillo-Rodriguez, L., Serruya, M. D., Herweg, N. A., Waldman, Z. J., Wanda, P. A., . . . Sperling, M. R. (2021). Contribution of left supramarginal and angular gyri to episodic memory encoding: An intracranial EEG study. *Neuroimage, 225*, 117514. doi:10.1016/j.neuroimage.2020.117514

Sacco, G., Ben-Sadoun, G., Bourgeois, J., Fabre, R., Manera, V., & Robert, P. (2019). Comparison between a Paper-Pencil Version and Computerized Version for the Realization of a Neuropsychological Test: The Example of the Trail Making Test. *J Alzheimers Dis, 68*(4), 1657-1666. doi:10.3233/jad-180396

Schaefer, A., Quinque, E. M., Kipping, J. A., Arélin, K., Roggenhofer, E., Frisch, S., . . . Schroeter, M. L. (2014). Early small vessel disease affects frontoparietal and cerebellar hubs in close correlation with clinical symptoms–a resting-state fMRI study. *J Cereb Blood Flow Metab, 34*(7), 1091-1095. doi:10.1038/jcbfm.2014.70

Shakil, S., Lee, C. H., & Keilholz, S. D. (2016). Evaluation of sliding window correlation performance for characterizing dynamic functional connectivity and brain states. *Neuroimage, 133*, 111-128. doi:10.1016/j.neuroimage.2016.02.074

Sibille, E., Morris, H. M., Kota, R. S., & Lewis, D. A. (2011). GABA-related transcripts in the dorsolateral prefrontal cortex in mood disorders. *Int J Neuropsychopharmacol, 14*(6), 721-734. doi:10.1017/s1461145710001616

Smith, E. E., Salat, D. H., Jeng, J., McCreary, C. R., Fischl, B., Schmahmann, J. D., . . . Greenberg, S. M. (2011). Correlations between MRI white matter lesion location and executive function and episodic memory. *Neurology, 76*(17), 1492-1499. doi:10.1212/WNL.0b013e318217e7c8

Sridharan D, L. D., Menon V. (2008). A critical role for the right fronto-insular cortex in switching between central-executive and default-mode networks. doi:10.1073/pnas.0800005105

Sridharan, D., Levitin, D. J., & Menon, V. (2008). A critical role for the right fronto-insular cortex in switching between central-executive and default-mode networks. *Proc Natl Acad Sci U S A, 105*(34), 12569-12574. doi:10.1073/pnas.0800005105

Torrens-Burton, A., Basoudan, N., Bayer, A. J., & Tales, A. (2017). Perception and Reality of Cognitive Function: Information Processing Speed, Perceived Memory Function, and Perceived Task Difficulty in Older Adults. *J Alzheimers Dis, 60*(4), 1601-1609. doi:10.3233/jad-170599

Tzourio-Mazoyer, N., Landeau, B., Papathanassiou, D., Crivello, F., Etard, O., Delcroix, N., . . . Joliot, M. (2002). Automated anatomical labeling of activations in SPM using a macroscopic anatomical parcellation of the MNI MRI single-subject brain. *Neuroimage, 15*(1), 273-289. Retrieved from http://www.ncbi.nlm.nih.gov/pubmed/11771995. doi:10.1006/nimg.2001.0978

van Leijsen, E. M. C., van Uden, I. W. M., Bergkamp, M. I., van der Holst, H. M., Norris, D. G., Claassen, J., . . . Tuladhar, A. M. (2019). Longitudinal changes in rich club organization and cognition in cerebral small vessel disease. *Neuroimage Clin, 24*, 102048. doi:10.1016/j.nicl.2019.102048

Wang, J., Wang, X., Xia, M., Liao, X., Evans, A., & He, Y. (2015). GRETNA: a graph theoretical network analysis toolbox for imaging connectomics. *Front Hum Neurosci, 9*, 386. doi:10.3389/fnhum.2015.00386

Wardlaw, J. M., Smith, E. E., Biessels, G. J., Cordonnier, C., Fazekas, F., Frayne, R., . . . Dichgans, M. (2013). Neuroimaging standards for research into small vessel disease and its contribution to ageing and neurodegeneration. *Lancet Neurol, 12*(8), 822-838. doi:10.1016/s1474-4422(13)70124-8

Wee, C. Y., Yang, S., Yap, P. T., & Shen, D. (2016). Sparse temporally dynamic resting-state functional connectivity networks for early MCI identification. *Brain Imaging Behav, 10*(2), 342-356. doi:10.1007/s11682-015-9408-2

Whitfield-Gabrieli, S., & Ford, J. M. (2012). Default mode network activity and connectivity in psychopathology. *Annu Rev Clin Psychol, 8*, 49-76. doi:10.1146/annurev-clinpsy-032511-143049

Yan, C. G., Cheung, B., Kelly, C., Colcombe, S., Craddock, R. C., Di Martino, A., . . . Milham, M. P. (2013). A comprehensive assessment of regional variation in the impact of head micromovements on functional connectomics. *Neuroimage, 76*, 183-201. doi:10.1016/j.neuroimage.2013.03.004

Yan, C. G., Wang, X. D., Zuo, X. N., & Zang, Y. F. (2016). DPABI: Data Processing & Analysis for (Resting-State) Brain Imaging. *Neuroinformatics, 14*(3), 339-351. doi:10.1007/s12021-016-9299-4

Figures

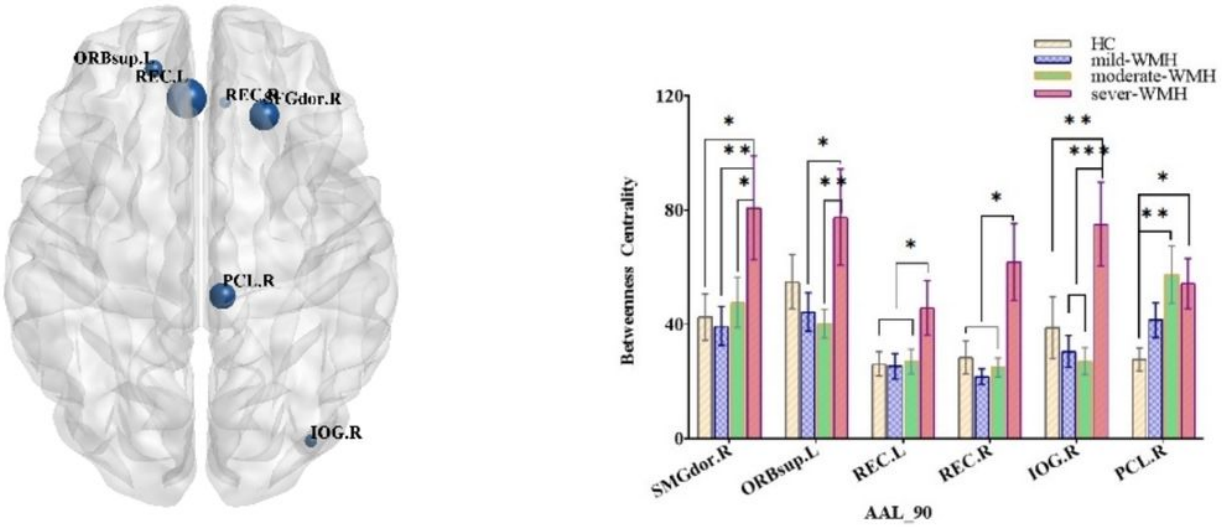

Figure 1

Group comparisons of betweenness centrality. Right rectus gyrus (REC.R), right inferior occipital lobe (IOG.R), right paracentral lobule (PCL.R), right dorsolateral superior frontal gyrus (SFGdor.R), left rectus gyrus (REC.L), and left orbital part of the superior frontal gyrus (ORBsup.R). *** significant at 0.001 level, ** significant at 0.01 level and * significant at 0.05 level (2-tailed).

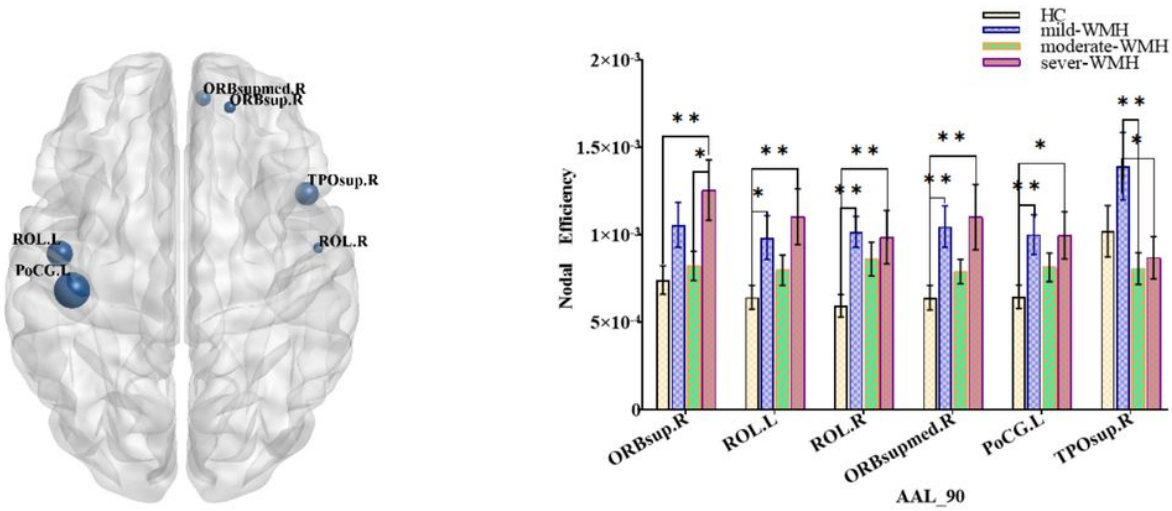

Figure 2

Group comparisons of nodal efficiency. Right rolandic operculum (ROL.R), right orbital part of superior frontal gyrus (ORBsup.R), right medial orbital part of superior frontal gyrus (ORBsupmed.R), right Temporal pole: superior temporal gyrus (TPOsup.R), left rolandic operculum (ROL.L), and left postcentral gyrus (PoCG.L). *** significant at 0.001 level, ** significant at 0.01 level and * significant at 0.05 level (2-tailed).

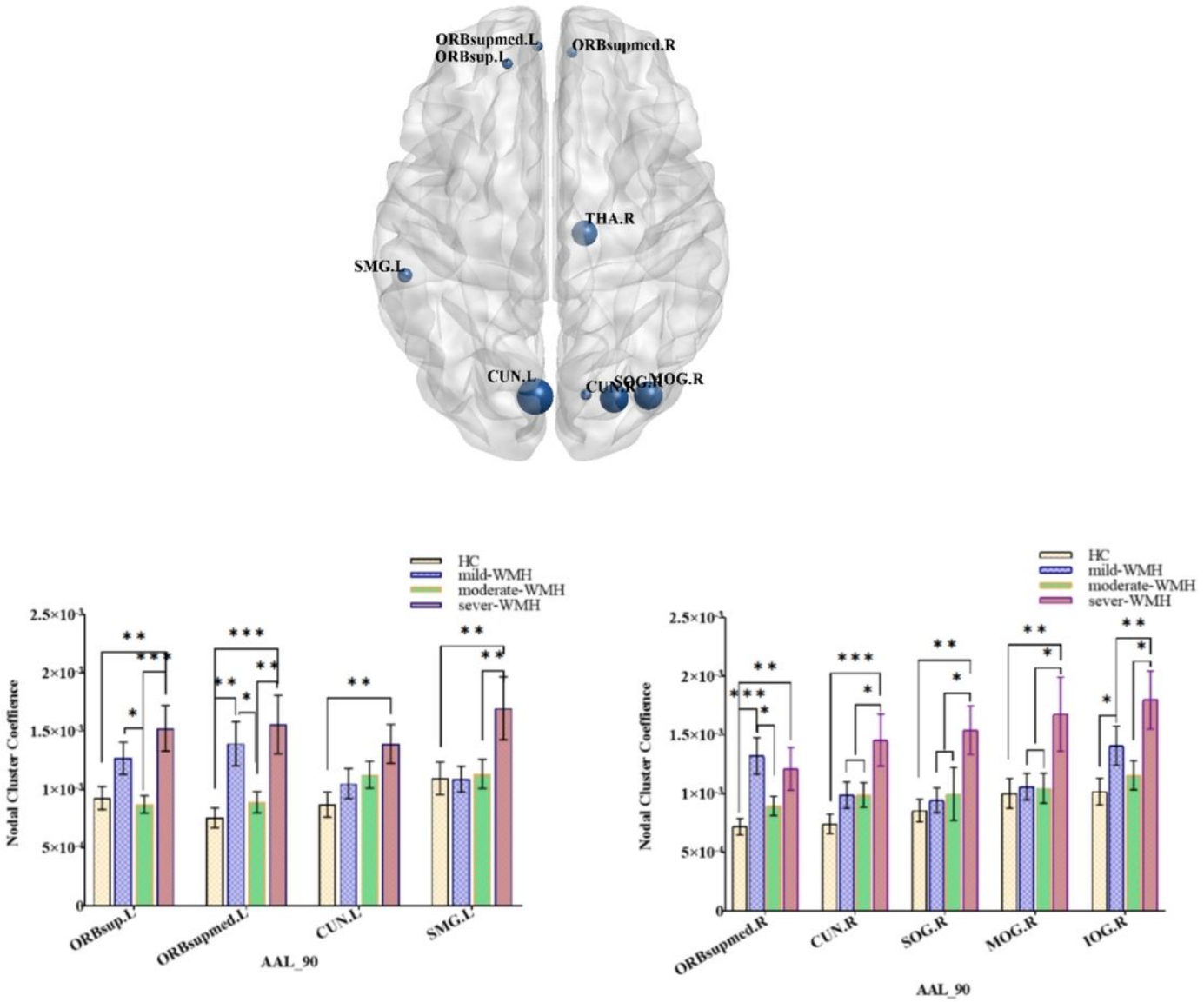

Figure 3

Group comparisons of the nodal cluster coefficiency. Right cuneus (CUN.R), right medial orbital part of superior frontal gyrus (ORBsupmed.R), right superior occipital gyrus (SOG.R), right middle occipital gyrus (MOG.R), right inferior occipital lobe (IOG.R), left cuneus (CUN.L), left medial orbital part of superior frontal gyrus (ORBsupmed.L), left orbital part of superior frontal gyrus (ORBsup.L), and left supramarginal gyrus (SMG.L). *** significant at 0.001 level, ** significant at 0.01 level and * significant at 0.05 level (2-tailed).

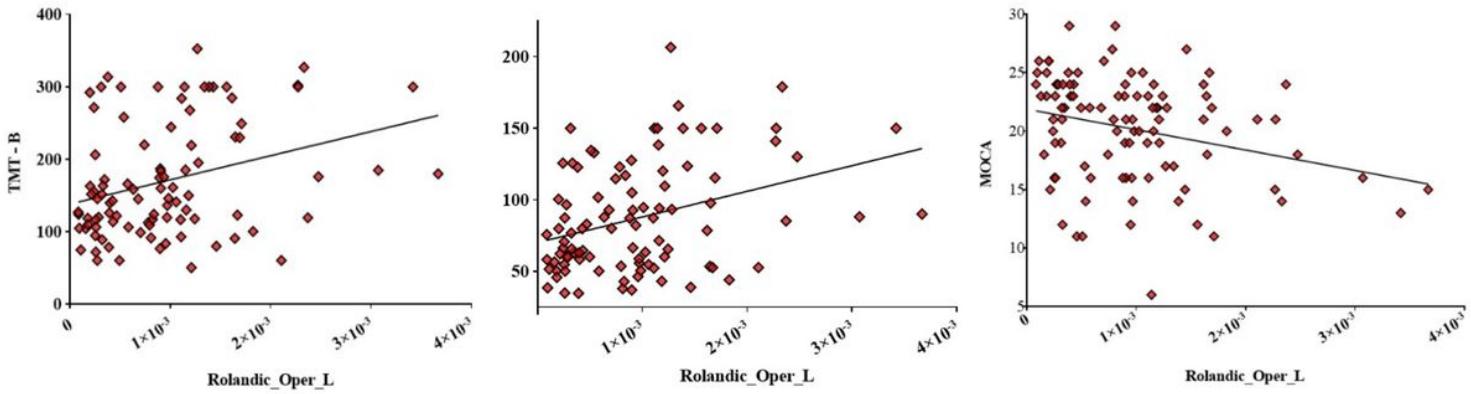

Figure 4

Correlations between the nodal efficiency of the left rolandic operculum and MoCA score, TMT-A time and TMT-B time in patients with WMHs. WMHs, white matter hyperintensities; MoCA, Montreal Cognitive Assessment; TMT, Trial Making Test.

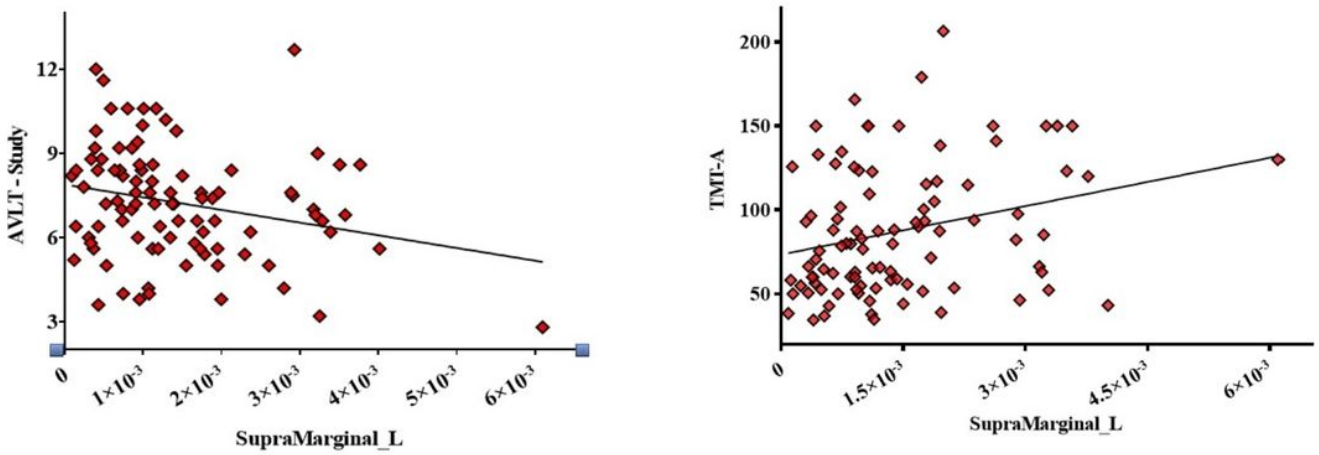

Figure 5

Correlations between the left supramarginal gyrus and TMT-A time and the score of AVLT-study in patients with WMHs. WMHs, white matter hyperintensities; AVLT, Chinese Auditory Learning Test; TMT, Trial Making Test.

Supplementary Files

This is a list of supplementary files associated with this preprint. Click to download.

- AuthorChecklist.pdf
- AuthorDeclarationForm.pdf